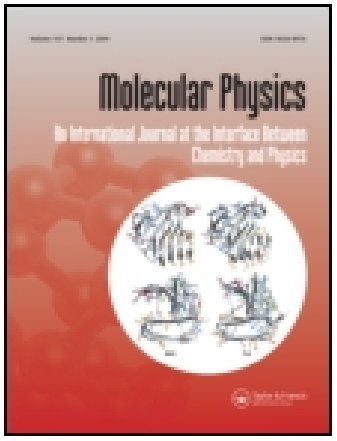

Molecular Physics: An International Journal at the Interface Between Chemistry and Physics
Publication details, including instructions for authors and subscription information:
http://www.tandfonline.com/loi/tmph20

Multiresolution quantum chemistry in multiwavelet bases: time-dependent density functional theory with asymptotically corrected potentials in local density and generalized gradient approximations

Takeshi Yanai [a] , Robert J. Harrison [a] & Nicholas C. Handy [b]
[a] Oak Ridge National Laboratory , PO Box 2008 MS6367, Oak Ridge TN 37831, USA
[b] Department of Chemistry , University of Cambridge , Cambridge, CB2 1EW, UK
[c] Oak Ridge National Laboratory , PO Box 2008 MS6367, Oak Ridge TN 37831, USA E-mail:
Published online: 21 Feb 2007.

To cite this article: Takeshi Yanai , Robert J. Harrison & Nicholas C. Handy (2005) Multiresolution quantum chemistry in multiwavelet bases: time-dependent density functional theory with asymptotically corrected potentials in local density and generalized gradient approximations, Molecular Physics: An International Journal at the Interface Between Chemistry and Physics, 103:2-3, 413-424, DOI: 10.1080/00268970412331319236

To link to this article: http://dx.doi.org/10.1080/00268970412331319236

Molecular Physics, Vol. 103, No. 2–3, 20 January–10 February 2005, 413–424

Multiresolution quantum chemistry in multiwavelet bases: time-dependent density functional theory with asymptotically corrected potentials in local density and generalized gradient approximations

TAKESHI YANAI†*, ROBERT J. HARRISON†* and NICHOLAS C. HANDY‡
†Oak Ridge National Laboratory, PO Box 2008 MS6367, Oak Ridge TN 37831, USA
‡Department of Chemistry, University of Cambridge, Cambridge, CB2 1EW, UK

(*Received 30 July 2004; in final form 25 August 2004*)

A multiresolution solver for fully numerical linear response calculations of excitation states via the time-dependent Hartree–Fock and density functional theory (TD-HF/DFT) is presented. The linear response method Yanai *et al*. previously reported [*J. Chem. Phys*., submitted] was limited to the Tamm–Dancoff approximation and could only use the Hartree–Fock exchange and the local-spin density approximation (LSDA) with a crude asymptotic correction. The present development enables us to perform full TD-HF/DFT calculations employing generalized gradient approximation (GGA) exchange-correlation potentials as well as hybrid ones. The linear response of TD-HF/DFT is computed by means of iteratively solving the coupled integral equations with the Green's functions. In this study, Tozer and Handy's asymptotic correction (AC) is applied to existing DFT exchange-correlations, and is found numerically stable and efficient. Furthermore, the new hybrid exchange-correlation functional CAM-B3LYP, which was recently proposed by Yanai *et al*. [*Chem. Phys. Lett*. **393,** 51 (2004)], is implemented. The implementation requires a new separated representation of the integral kernel for the Coulomb-attenuated potential. We demonstrate linear response calculations free of basis set error for the excited states of Be, N_2, C_2H_4 and C_6H_6 using LSDA, HCTH, CAM-B3LYP and PBE0 exchange-correlation functionals. The mean absolute errors of the C_6H_6 calculations with HCTH and CAM-B3LYP are 0.12 and 0.18 eV, respectively. The second derivative of exchange-correlation functionals is represented fully numerically at $O(N)$ computation cost.

1. Introduction

Recently, we introduced a multiresolution approach to quantum chemistry in multiwavelet bases [1]. It was demonstrated to reproduce basis function limit predictions for Hartree–Fock and Kohn–Sham calculations [2–5]. It is important to demonstrate the wide applicability of this new approach. Here we apply the multiresolution approach to the time-dependent Hartree–Fock (TDHF) theory and time-dependent density functional theory (TDDFT) for the calculation of the energies of excited states.

There are several new aspects in this present paper. (i) We do not use the Tamm–Dancoff approximation, i.e. in the perturbation equations we include terms involving $\exp(i\omega t)$ and $\exp(-i\omega t)$; this is in contrast to our earlier implementation [2]. (ii) We use both GGA and hybrid functionals, and we fully include the derivatives of these functionals in the equations, i.e. we do not substitute the LDA approximation. (iii) We introduce the Tozer–Handy asymptotic correction (AC) [6] to the exchange-correlation potential to ensure that excitations to Rydberg states are properly calculated. (iv) We introduce our new CAM-B3LYP functional [7] and examine its performance, in conjunction with the AC correction as appropriate; this is important as we have already shown that it overcomes many of the outstanding weaknesses of DFT.

We present results using LDA, HCTH, PBE0, CAM-B3LYP functionals and we compare them with previous calculations using HCTH, BLYP and *ab initio* methodology, for the molecules H_2, Be, N_2, C_2H_4 and C_6H_6. The theory of multieresolution linear response is introduced in the next section.

* Corresponding authors. Email: yanait@ornl.gov (TY); harrisonrj@ornl.gov (RJH)

Molecular Physics
ISSN 0026–8976 print/ISSN 1362–3028 online © 2005
Taylor & Francis Group Ltd
http://www.tandf.co.uk/journals
DOI: 10.1080/00268970412331319236

2. Method

2.1. *Integral equations of time-dependent density functional theory*

In a previous linear response paper for the HF/DFT method [2], we derived the following coupled eigen-equations for the full TD-HF/DFT method for the response functions $\{x_p\}$, $\{y_p\}$, $p = 1, \ldots, n_{\mathrm{occ}}$ and the excitation energy ω as

$$\left(1-\hat{\rho}^0\right)\left[\left(\hat{F}^0-\epsilon_p^0\right)x_p(r)+\left\{\frac{\partial\hat{g}}{\partial\rho}\left[\rho^0\right]*\rho'(r,r')\right\}\phi_p(r)\right] = \omega x_p(r), \tag{1}$$

$$\left(1-\hat{\rho}^0\right)^\dagger\left[\left(\hat{F}^0-\epsilon_p^0\right)^\dagger y_p(r)+\left\{\frac{\partial\hat{g}}{\partial\rho}\left[\rho^0\right]*\rho'(r,r')\right\}^\dagger\phi_p(r)\right] = -\omega y_p(r), \tag{2}$$

where $\rho^0(r,r')$ is the density matrix, $\hat{F}^0$ is the Fock operator, $\phi_p(r)$ and ϵ_p^0 are the occupied orbitals and their energies, respectively, and $\hat{g}[\rho]$ is the electron-interaction operator, and

$$\rho'(r,r') = \sum_i^{\mathrm{occ}} x_i(r)\phi_i^\dagger(r') + \sum_i^{\mathrm{occ}} \phi_i(r)y_i^\dagger(r'), \tag{3}$$

which is termed the transition density matrix. From the above equations, the relation $\hat{F}^0 = -\nabla^2/2 + \hat{V}^0$ yields working integral equations as follows:

$$x_p(r) = -2\hat{G}(k_x) * \left[\hat{V}^0 x_p(r) + \left(1-\hat{\rho}^0\right)\hat{\Gamma}\phi_p(r)\right], \tag{4}$$

$$y_p(r) = -2\hat{G}(k_y) * \left[\hat{V}^0 y_p(r) + \left(1-\hat{\rho}^0\right)\hat{\Gamma}^\dagger\phi_p(r)\right], \tag{5}$$

where $\hat{G}$ is the integral operator with the kernel being the Green's function and the electron interaction term is replaced with $\hat{\Gamma}$ as

$$\hat{\Gamma} = \frac{\partial\hat{g}}{\partial\rho}\left[\rho^0\right] * \rho'(r,r'). \tag{6}$$

The kernel for the integral operator $\hat{G}$ is parametrized with $k_x = [-2(\epsilon_p^0+\omega)]^{1/2}$ and $k_y = [-2(\epsilon_p^0-\omega)]^{1/2}$. The current implementation can use the bound-state Helmholtz (BSH) kernel as well as the Poisson kernel for the Green's function in three dimensions, which was developed in a previous study [1]. The eigenfunctions and eigenvalues $\{x_p\}$, $\{y_p\}$ and ω are determined by iterating the integral equations (equations (4) and (5)).

2.2. *Expressions for the electron interaction term*

The specific expressions of the electron interaction term $\hat{\Gamma}$ for Coulomb, Hartree–Fock exchange and exchange correlation functional are follows.

(1) Coulomb operator:

$$\hat{\Gamma}\phi_p(r) = \left(\int \mathrm{d}r' \frac{\rho'(r',r')}{|r-r'|}\right)\phi_p(r). \tag{7}$$

(2) Hartree–Fock exchange operator:

$$\hat{\Gamma}\phi_p(r) = \left(\sum_i^{\mathrm{occ}} x_i(r)\int \mathrm{d}r' \frac{\phi_i^\dagger(r')\phi_p(r')}{|r-r'|}\right) + \left(\sum_i^{\mathrm{occ}} \phi_i(r)\int \mathrm{d}r' \frac{y_i^\dagger(r')\phi_p(r')}{|r-r'|}\right), \tag{8}$$

$$\hat{\Gamma}^\dagger\phi_p(r) = \left(\sum_i^{\mathrm{occ}} \phi_i(r)\int \mathrm{d}r' \frac{x_i^\dagger(r')\phi_p(r')}{|r-r'|}\right) + \left(\sum_i^{\mathrm{occ}} y_i(r)\int \mathrm{d}r' \frac{\phi_i^\dagger(r')\phi_p(r')}{|r-r'|}\right). \tag{9}$$

(3) DFT exchange-correlation potential:

$$\hat{\Gamma}\phi_p(r) = \left\{\frac{\partial^2 E_{\mathrm{xc}}}{\partial\rho^2}\left[\rho^0\right] * \rho'(r)\right\}\phi_p(r). \tag{10}$$

In the local spin density approximation (LSDA) and generalized gradient approximation (GGA), the exchange-correlation energy is a functional of the density function and its gradient invariants γ as

$$E_{\mathrm{xc}} = \int \mathrm{d}r f_{\mathrm{xc}}\left(\rho_\alpha^0, \rho_\beta^0, \gamma_{\alpha\alpha}^0, \gamma_{\alpha\beta}^0, \gamma_{\beta\beta}^0\right), \tag{11}$$

which leads to the corresponding exchange-correlation potential,

$$v_{\mathrm{xc}} = \frac{\delta E_{\mathrm{xc}}}{\delta\rho_\alpha} = \frac{\partial f_{\mathrm{xc}}}{\partial\rho_\alpha} - 2\nabla\cdot\left(\frac{\partial f_{\mathrm{xc}}}{\partial\gamma_{\alpha\alpha}}\nabla\rho_\alpha^0\right) - \nabla\cdot\left(\frac{\partial f_{\mathrm{xc}}}{\partial\gamma_{\alpha\beta}}\nabla\rho_\beta^0\right), \tag{12}$$

where $\rho^0 = \rho^0_\alpha + \rho^0_\beta$. The second-derivative terms in equation (11) are derived as

$$\begin{aligned}\frac{\partial^2 E_{\mathrm{xc}}}{\partial\rho_\alpha^2}\left[\rho^0\right] * \rho' &= \frac{\partial^2 f_{\mathrm{xc}}}{\partial\rho_\alpha^2}\rho' + 2\frac{\partial^2 f_{\mathrm{xc}}}{\partial\rho_\alpha\partial\gamma_{\alpha\alpha}}(\nabla\rho_\alpha\cdot\nabla\rho') \\ &+ \frac{\partial^2 f_{\mathrm{xc}}}{\partial\rho_\alpha\partial\gamma_{\alpha\beta}}(\nabla\rho_\beta\cdot\nabla\rho') \\ &- \nabla\cdot\left((\nabla\rho_\alpha)\left\{2\frac{\partial^2 f_{\mathrm{xc}}}{\partial\rho_\alpha\partial\gamma_{\alpha\alpha}}\rho' + 4\frac{\partial^2 f_{\mathrm{xc}}}{\partial\gamma_{\alpha\alpha}^2}(\nabla\rho_\alpha\cdot\nabla\rho')\right.\right. \\ &\qquad \left.\left. + 2\frac{\partial^2 f_{\mathrm{xc}}}{\partial\gamma_{\alpha\alpha}\partial\gamma_{\alpha\beta}}(\nabla\rho_\beta\cdot\nabla\rho')\right\}\right) \\ &- \nabla\cdot\left((\nabla\rho_\beta)\left\{\frac{\partial^2 f_{\mathrm{xc}}}{\partial\rho_\alpha\partial\gamma_{\alpha\beta}}\rho'\right.\right. \\ &\qquad \left.\left. + 2\frac{\partial^2 f_{\mathrm{xc}}}{\partial\gamma_{\alpha\alpha}\partial\gamma_{\alpha\beta}}(\nabla\rho_\alpha\cdot\nabla\rho') + \frac{\partial^2 f_{\mathrm{xc}}}{\partial\gamma_{\alpha\beta}^2}(\nabla\rho_\beta\cdot\nabla\rho')\right\}\right) \\ &- \nabla\cdot\left(2\frac{\partial f_{\mathrm{xc}}}{\partial\gamma_{\alpha\alpha}}\nabla\rho'\right), \end{aligned} \tag{13}$$

$$\begin{aligned}\frac{\partial^2 E_{\mathrm{xc}}}{\partial\rho_\alpha\partial\rho_\beta}\left[\rho^0\right] * \rho' &= \frac{\partial^2 f_{\mathrm{xc}}}{\partial\rho_\alpha\partial\rho_\beta}\rho' + \frac{\partial^2 f_{\mathrm{xc}}}{\partial\rho_\alpha\partial\gamma_{\alpha\beta}}(\nabla\rho_\alpha\cdot\nabla\rho') \\ &+ 2\frac{\partial^2 f_{\mathrm{xc}}}{\partial\rho_\alpha\partial\gamma_{\beta\beta}}(\nabla\rho_\beta\cdot\nabla\rho') \\ &- \nabla\cdot\left((\nabla\rho_\alpha)\left\{2\frac{\partial^2 f_{\mathrm{xc}}}{\partial\rho_\beta\partial\gamma_{\alpha\alpha}}\rho'\right.\right. \\ &\qquad \left.\left. + 2\frac{\partial^2 f_{\mathrm{xc}}}{\partial\gamma_{\alpha\alpha}\partial\gamma_{\alpha\beta}}(\nabla\rho_\alpha\cdot\nabla\rho') + 4\frac{\partial^2 f_{\mathrm{xc}}}{\partial\gamma_{\alpha\alpha}\partial\gamma_{\beta\beta}}(\nabla\rho_\beta\cdot\nabla\rho')\right\}\right) \\ &- \nabla\cdot\left((\nabla\rho_\beta)\left\{\frac{\partial^2 f_{\mathrm{xc}}}{\partial\rho_\beta\partial\gamma_{\alpha\beta}}\rho' + \frac{\partial^2 f_{\mathrm{xc}}}{\partial\gamma_{\alpha\beta}^2}(\nabla\rho_\alpha\cdot\nabla\rho')\right.\right. \\ &\qquad \left.\left. + 2\frac{\partial^2 f_{\mathrm{xc}}}{\partial\gamma_{\alpha\beta}\partial\gamma_{\beta\beta}}(\nabla\rho_\beta\cdot\nabla\rho')\right\}\right) \\ &- \nabla\cdot\left(\frac{\partial f_{\mathrm{xc}}}{\partial\gamma_{\alpha\beta}}\nabla\rho'\right). \end{aligned} \tag{14}$$

The conventional formulation of the second-derivative exchange-correlation term in the finite basis expansion approach takes the four-centred integral [6, 8], whereas our approach computes fully numerical representations of equations (13) and (14) in three-dimensional coordinates. The numerical computation is carried out literally according to the arithmetic expressions of equations (13) and (14), which involves the multiplications of functions and the applications of the differentiation operator to functions. The total computations go through one-centred (local) numerical operations upon the density function $\rho^0(r)$ and the transition density function $\rho'(r)$. Therefore, the computational cost required is $O(N)$. The details on the implementation of GGA functionals in the multiresolution solver is reported in [5].

2.3. *Asymptotic correction to the extant exchange-correlation potentials*

The current implementation for the integral operator enables us to use the Poisson kernel and the bound-state Helmholtz (BSH) kernel for the Green's function. We can presently only use the real numbers for the parameters k_x and k_y of the integral operators in equations (4) and (5), so that the resulting orbitals and response functions should be bound, and, concomitantly, the relation $\epsilon^0_{\mathrm{HOMO}} \le \omega \le -\epsilon^0_{\mathrm{HOMO}}$ has to be satisfied. In our previous linear response study [2], we reported that the correct asymptotic behaviour $1/r$ in the exchange-correlation potential is essential for TDDFT response calculations free of basis errors in order to yield the bound states through the integral equation. In the study, we applied Hirata's asymptotic correction (AC) [8] to LSDA [9] exchange-correlation potential. Hirata's AC introduces the correct asymptotic behaviour via the Slater potential and shifts down the potential so that the HOMO energy corresponds to the ionization potential. Although the approach succeeded in introducing the asymptotic behaviour in the existing exchange-correlation potentials, it has a numerical difficulty in computing the Slater potential numerically, which involves the density function in the denominator.

Tozer and Handy proposed an AC method [6, 10], which enforces the following asymptotic form to the existing exchange-correlation potentials,

$$v_{\mathrm{xc}}^{\mathrm{AC}}(r) \to -\frac{1}{r} + I + \epsilon_{\mathrm{h}}, \tag{15}$$

where I is the ionization potential and ϵ_{h} is the highest occupied Kohn–Sham eigenvalue. For computational reasons, they represented the first term of the right-hand side of equation (15) by a truncated multipole expansion. They demonstrated that their AC approach greatly improves the results for excitations to Rydberg states of TDDFT calculations. Their observation was that their asymptotically corrected potential leads to significantly improved virtual orbitals and eigenvalues.

We have found that this AC approach can be easily implemented in our numerical TDDFT code and is numerically stable. Since we do not take virtual orbitals explicitly in the multiresolution solver, we shift down Tozer and Handy's potential by $I + \epsilon_{\mathrm{h}}$ so that we have an asymptotic behaviour as $v_{\mathrm{xc}}^{\mathrm{AC}}(r) \to -1/r$ at the

large r, instead of equation (15). The overall exchange-correlation potential is given by

$$v_{\mathrm{xc}}^{\mathrm{LDA/GGA\,(AC)}}(r) = \begin{cases} v_{\mathrm{xc}}^{\mathrm{LSDA/GGA}}(r) - I - \epsilon_{\mathrm{h}}, & (r_{\mathrm{A}} < X\sigma_{\mathrm{A}}, \text{ for any A}), \\ -\dfrac{1}{N}\displaystyle\sum_{\mathrm{A}} \frac{Q_{\mathrm{A}}}{r_{\mathrm{A}}} \left(\simeq -\frac{1}{r}\right), & (r_{\mathrm{A}} > Y\sigma_{\mathrm{A}}, \forall \mathrm{A}), \\ \text{intermediate}, & (\text{otherwise}), \end{cases} \tag{16}$$

where $v_{\mathrm{xc}}^{\mathrm{LSDA/GGA}}(r)$ is the standard LSDA or GGA exchange-correlation potential, r_{A} is the distance between r (the electron coordinate) and atom A, σ_{A} is the Bragg–Slater radius, N is the number of atoms, Q_{A} is atomic charge and X, Y are the numerical parameters to partition the spatial position into the non-AC and AC regions. The potential at the intermediate region connects smoothly between non-AC and AC potentials [6].

2.4. *CAM-B3LYP exchange-correlation functional*

Very recently, two of the authors (TY and NCH) and Tew proposed a new hybrid exchange-correlation functional CAM-B3LYP [7], which combines the hybrid qualities of B3LYP [11, 12] and the long-range correction (LC) [13, 14]. We demonstrated that the CAM-B3LYP yields atomization energies of similar quality to those from B3LYP, while also performing well for charge transfer excitations in a dipeptide model, which B3LYP underestimates enormously. The CAM-B3LYP is derived from the following Coulomb-Attenuating Method (CAM) split of the electron interaction term r_{12}^{-1} with three parameters α, β and μ,

$$\frac{1}{r_{12}} = \frac{1 - [\alpha + \beta \operatorname{erf}(\mu r_{12})]}{r_{12}} + \frac{\alpha + \beta \operatorname{erf}(\mu r_{12})}{r_{12}}. \tag{17}$$

The above form determines the blend of the DFT exchange (via the first term) and the HF exchange (via the last term) at r_{12}. Our best functional with $\alpha = 0.19$, $\alpha + \beta = 0.65$, $\mu = 0.33$ comprises of 0.19 HF plus 0.81 Becke 1988 (B88) exchange interaction at short range, and 0.65 HF plus 0.35 B88 exchange interaction at long range. The details are described in [7].

The important addition, which enables us to use the CAM-B3LYP in the multiresolution solver, is to construct a separated representation of the Green's function for the attenuated Poisson kernel (i.e. the last term of equation (17)). According to a previous paper [1], which presented an elaborate separation approach for the Poisson and BSH kernels, at first we derive the following integral representation,

$$\frac{\alpha + \beta \operatorname{erf}(\mu r_{12})}{r_{12}} = (\alpha + \beta) \int_{-\infty}^{\log \mu} \exp[-r^2 \exp(2s) + s]\, \mathrm{d}s + \alpha \int_{\log \mu}^{\infty} \exp[-r^2 \exp(2s) + s]\, \mathrm{d}s, \tag{18}$$

then discretize it with Gaussian functions on two intervals $[s_{\min}, \log \mu]$ and $[\log \mu, s_{\max}]$ using the trapezoidal rule. The notable numerical error arises at $s_\mu = \log \mu$ (the discontinuous point) on the above numerical integration. It can be corrected according to the Euler–Maclaurin summation formula [15], so that a scheduled accuracy is derived by using the following correction term up to the kth expansion,

$$-\beta \left[\frac{B_2}{2!} h^2 f'(s_\mu) + \cdots + \frac{B_{2k}}{(2k)!} h^{2k} f^{(2k-1)}(s_\mu) \right] + o(\epsilon_{2k}), \tag{19}$$

where h is the size of the subintervals of the numerical integration, B_{2k} are Bernoulli numbers, $f(s) = \exp[-r^2 \exp(2s) + s]$ and

$$\epsilon_{2k} = \frac{B_{2k+2}}{(2k+2)!} h^{2k+3} \max \left\| f^{(2k+2)}(s) \right\|. \tag{20}$$

The derivatives of $f(s_\mu)$ in equation (19) are calculated numerically using the Lagrangian polynomial interpolation on sufficient grid points around s_μ so as to yield the desired accuracy. The grid points are taken from those used in the trapezoidal numerical integration of equation (18).

Furthermore, we incorporate Tozer and Handy's AC into the CAM-B3LYP exchange-correlation potential. This is because the potential of the CAM-B3LYP behaves asymptotically not as $-1/r$, but as $-(\alpha + \beta)/r$, which comes exclusively from the HF exchange term, and the HOMO energy is underestimated with comparison to the ionization potential. Thus we modify the DFT (i.e. non-HF) exchange-correlation part $v_{\mathrm{xc}}^{\mathrm{LSDA/GGA}}(r)$ in CAM-B3LYP, using the asymptotic correction of equation (16), where its DFT potential in the asymptotic region (i.e. at $r_{\mathrm{A}} > Y\sigma_{\mathrm{A}}$, $\forall$A) is scaled by $1 - (\alpha + \beta)$ so that it behaves asymptotically as $-[1 - (\alpha + \beta)]/r$.

3. Result

3.1. *TD-HF, TD-LSDA, TD-HCTH calculations for hydrogen molecule*

Initial molecular calculations of TD-HF/DFT (without Tamm–Dancoff approximation) were performed on the

hydrogen molecule ($r = 1.4$ bohr). The LSDA [9] and HCTH [16] exchange-correlation functionals were employed for TDDFT calculations. We used both the non-AC (standard) and AC exchange-correlation functionals in the multiresolution TDDFT calculations. Table 1 lists the low-lying triplet excitation energies along with the total and HOMO energies and the ionization potentials. The molecular orbitals and response functions represented with 7th and 9th order multiwavelet bases, noted by $k = 7$ and $k = 9$, respectively, meet the convergence criteria where their residuals r(MO) are less than 3×10^{-4} ($k = 7$), 3×10^{-5} ($k = 7$) and 3×10^{-6} ($k = 9$). The box size was set as 200 bohr and the nuclear potentials smoothed so that the error in the total energy was accurate to 10^{-6} hartree, denoted as $\epsilon_{\text{nuc}} = 10^{-6}$ hereafter. The two parameters for the AC, X and Y in equation (16), are chosen as $X = 3.0$ and $Y = 4.0$. The table includes Gaussian calculations with aug-cc-pVTZ, aug-cc-pVQZ and d-aug-cc-pVQZ [17] using the NWChem program package [18]. Note that the TDDFT calculation with the AC exchange-correlation functionals was not carried out in Gaussian basis sets.

Overall, the multiresolution calculations yield the desired and consistent accuracy at the lowest excitation through the higher excitations including Rydberg states. With comparison to the most accurate results with $k = 9$ and $r(\text{MO}) < 3 \times 10^{-6}$, the accuracy attained in the multiresolution calculations is 10^{-3} eV for $k = 7$ and $r(\text{MO}) < 3 \times 10^{-4}$ and 10^{-4} eV for $k = 7$ and $r(\text{MO}) < 3 \times 10^{-5}$. As for Gaussian calculations, we observed that the basis errors of the lower excitation energies for TD-HF/DFT are around 10^{-2} eV, whereas, from the TDHF results, those of the higher-lying excitation energies are much larger. For instance, the errors of the $^3\Pi_g$ Rydberg state with aug-cc-pVTZ, aug-cc-pVQZ and d-aug-cc-pVQZ are 3.1, 2.1 and 0.15 eV, respectively.

The four higher-lying excitation states $^3\Pi_u$, $2^3\Sigma_u$, $2^3\Sigma_g$ and $^3\Pi_g$ computed with non-AC LSDA and HCTH are unbound states. Their excitation energies calculated with Gaussian basis sets are highly dependent on the diffuse functions and are approaching toward the HOMO orbital energies ($\epsilon_{\text{h}} = 10.3$ eV (LSDA) and 10.5 eV (HCTH)) with larger, more augmented basis sets.

The AC successfully yields the bound results for the higher-lying states in the multiresolution TDDFT calculations. We did not have any numerical difficulties in using the AC approach.

3.2. *TDDFT excitation energies for Be atom, N_2 and C_2H_4 molecules*

We performed TDDFT calculations on the Be atom, and the N_2 and C_2H_4 molecules. Tables 2, 3 and 4 show the total and HOMO energies without and with AC, and the ionization potentials without AC. The excitation energies are summarized in tables 5, 6 and 7. The tables include the literature Gaussian results reported by Hirata *et al.* [8] and Tozer and Handy [6, 23] together with experimental data and the results calculated by the accurate *ab initio* methods. The present calculations were performed with the 7th order multiwavelets, the residuals of MOs and response functions were less than 3×10^{-5}, using the LSDA, HCTH, CAM-B3LYP and PBE0 [24] exchange-correlation functionals. The box size was set as 200 bohr and the nuclear potential was smoothed with $\epsilon_{\text{nuc}} = 10^{-6}$. The core orbitals are frozen for the linear response calculations of Be and N_2. For the C_2H_4 molecule, only excitation from the highest valance π orbitals is considered.

Not surprisingly, the effect of the asymptotic correction on the total energies presented in tables 2, 3 and 4 is very small. The shifting down of the potentials satisfactorily improves the HOMO energies so that they nearly reproduce the ionization potentials. In the non-AC calculations, the CAM-B3LYP yields the lowest HOMO energies of all the functionals examined, due to the long-range correction through the HF exchange in the CAM approach. Comparing the multiresolution results with Tozer and Handy's results of the asymptotically corrected HCTH [6, 23] using augmented Sadlej triple zeta basis, their ionization potentials of the N_2 and C_2H_4 molecules were computed with the errors less than 2×10^{-3} hartree, even though the errors of the total energies are 3×10^{-2} hartree. This shows that the energy differences in the Gaussian calculations can be computed with higher precision than the total energies, because of the cancellation of inner-shell errors.

The excitation energies are numerically reliably and stably computed in the multiresolution calculations. The multiresolution results computed with HCTH accord with those reported by Tozer and Handy [6, 23] with the same functional. Overall, with comparison to the experimental data, the mean absolute errors of the TDDFT excitation energies are observed to be between 0.1 and 0.4 eV.

In the Be calculations, we used the same parameters $X = 3.0$ and $Y = 4.0$ for equation (16) as Tozer and Handy used and recommended in [23] rather than using $X = 3.5$ and $Y = 4.7$ as originally proposed in [6]. The CAM-B3LYP yields the smallest mean absolute errors and maximum absolute errors to the experimental data as 0.26 and 0.69 eV, respectively. Note that two states ^{1}D ($2p^2$) and ^{3}P ($2p^2$) are double excitations, which essentially cannot be described in the linear response calculations.

As for the N_2 calculations, we used two kinds of asymptotically corrected HCTH with the original

Table 1. The total, HOMO (ϵ_h) energies, ionization potential (I) (in hartree) and the low-lying triplet excitation energies (in eV) of H_2 molecule.

		Total energy	I	ϵ_h	$1^3\Sigma_u$	$1^3\Sigma_g$	$^3\Pi_u$	$2^3\Sigma_u$	$2^3\Sigma_g$	$^3\Pi_g$
HF	aug-cc-pVTZ	−1.133 026 8	0.563 572	−0.594 401	9.552 03	11.957 64	12.809 87	14.356 20	16.983 59	17.736 27
	aug-cc-pVQZ	−1.133 473 0	0.563 627	−0.594 615	9.552 87	11.960 97	12.589 55	14.290 50	16.321 08	16.786 09
	d-aug-cc-pVQZ	−1.133 476 6	0.563 631	−0.594 613	9.552 32	11.959 06	12.263 88	14.145 01	14.490 83	14.808 86
	$k = 7, r(\mathrm{MO}) < 3 \times 10^{-4}$	−1.133 629 7	0.563 646	−0.594 671	9.551 98	11.955 30	12.261 10	14.113 23	14.484 99	14.655 56
	$k = 7, r(\mathrm{MO}) < 3 \times 10^{-5}$	−1.133 629 7	0.563 646	−0.594 658	9.551 78	11.954 91	12.260 81	14.112 87	14.484 64	14.655 21
	$k = 9, r(\mathrm{MO}) < 3 \times 10^{-6}$	−1.133 629 8	0.563 646	−0.594 658	9.551 76	11.954 90	12.260 81	14.112 87	14.484 61	14.655 21
LSDA	aug-cc-pVTZ	−1.136 882 2	0.596 537	−0.377 159	9.934 76	10.651 52	12.457 10	12.399 97	15.759 51	16.368 61
	aug-cc-pVQZ	−1.137 332 7	0.596 662	−0.377 360	9.936 57	10.608 94	12.067 56	12.096 47	14.851 20	15.216 49
	d-aug-cc-pVQZ	−1.137 334 2	0.596 663	−0.377 355	9.927 25	10.305 24	10.942 29	10.715 75	11.190 99	11.979 38
	$k = 7, r(\mathrm{MO}) < 3 \times 10^{-4}$	−1.137 481 0	0.596 681	−0.377 376	9.926 70	10.260 78				
	$k = 7, r(\mathrm{MO}) < 3 \times 10^{-5}$	−1.137 481 0	0.596 681	−0.377 380	9.926 84	10.260 88				
	$k = 9, r(\mathrm{MO}) < 3 \times 10^{-6}$	−1.137 481 0	0.596 681	−0.377 374	9.927 38	10.260 72				
LSDA(AC)	$k = 7, r(\mathrm{MO}) < 3 \times 10^{-4}$	−1.137 318 0	0.596 532	−0.590 651	10.528 04	12.259 99	12.355 35	14.111 68	14.454 33	14.532 94
	$k = 7, r(\mathrm{MO}) < 3 \times 10^{-5}$	−1.137 317 5	0.596 531	−0.590 640	10.527 88	12.259 64	12.355 12	14.111 42	14.454 03	14.532 65
	$k = 9, r(\mathrm{MO}) < 3 \times 10^{-6}$	−1.137 317 4	0.596 531	−0.590 633	10.528 67	12.259 47	12.354 89	14.111 39	14.453 83	14.532 44
HCTH	aug-cc-pVTZ	−1.186 944 1	0.588 811	−0.385 019	10.191 43	10.793 64	12.740 36	12.706 95	15.849 14	16.298 00
	aug-cc-pVQZ	−1.187 323 7	0.588 714	−0.385 182	10.191 61	10.760 70	12.280 72	12.421 04	14.888 69	15.135 47
	d-aug-cc-pVQZ	−1.187 324 4	0.588 714	−0.385 180	10.180 66	10.517 47	11.119 73	10.950 05	11.357 86	12.227 89
	$k = 7, r(\mathrm{MO}) < 3 \times 10^{-4}$	−1.187 472 1	0.588 747	−0.385 190	10.186 83	10.474 25				
	$k = 7, r(\mathrm{MO}) < 3 \times 10^{-5}$	−1.187 472 1	0.588 747	−0.385 185	10.186 63	10.474 09				
	$k = 9, r(\mathrm{MO}) < 3 \times 10^{-6}$	−1.187 472 2	0.588 747	−0.385 185	10.186 40	10.474 03				
HCTH(AC)	$k = 7, r(\mathrm{MO}) < 3 \times 10^{-4}$	−1.187 315 6	0.588 598	−0.588 772	10.868 57	12.403 02	12.491 58	14.097 57	14.444 11	14.499 55
	$k = 7, r(\mathrm{MO}) < 3 \times 10^{-5}$	−1.187 315 6	0.588 598	−0.588 613	10.865 12	12.398 42	12.487 63	14.093 36	14.439 72	14.495 24
	$k = 9, r(\mathrm{MO}) < 3 \times 10^{-6}$	−1.187 315 4	0.588 598	−0.588 629	10.865 51	12.398 85	12.487 88	14.093 78	14.440 17	14.495 68

Table 2. The total, HOMO (ϵ_h) energies, and ionization potential (I) (in hartree) of Be.

	$k = 7, r(\mathrm{MO}) < 3 \times 10^{-5}$[a]				Hirata *et al.*[b]		
	LSDA	HCTH	CAM-B3LYP	PBE0	SVWN	BLYP	Exptl.[c]
Total energy	−14.447 207	−14.669 387	−14.650 386	−14.636 639	−14.447 1	−14.661 4	–
ϵ_h	−0.205 734	−0.205 565	−0.282 047	−0.238 589	−0.205 7	−0.200 9	–
I	0.331 697	0.333 348	0.334 760	0.329 687	–	–	0.342 6
Total energy (AC)	−14.447 196	−14.669 356	−14.650 378	−14.636 634	14.447 1	14.661 4	–
$\epsilon_{h(AC)}$	−0.331 180	−0.332 398	−0.334 390	−0.329 378	−0.307 7	−0.309 3	–

[a] The asymptotic correction uses $X = 3.0$, $Y = 4.0$ for equation (16).
[b] From [8]. The basis: 16s11p7d GTOs.
[c] From [19].

and revised parameters of X and Y. Tozer and Handy's HCTH results were computed with the original parameters $Y = 3.5$ and $Y = 4.7$ [6]. We have found that the HCTH with the revised parameters $X = 3.0$ and $Y = 4.0$ produces better results than those with the original parameters, especially for the higher-lying Rydberg states.

The excitation energies of the C_2H_4 molecule computed with TDDFT are in excellent agreement with the experimental data. The mean absolute errors are 0.34, 0.11, 0.10 and 0.10 eV for LSDA, HCTH, CAM-B3LYP and PBE0, respectively. We used the parameters $X = 3.0$ and $Y = 4.0$ for the asymptotic correction, whereas Tozer and Handy's calculations were performed with $X = 3.5$ and $Y = 4.7$ [6].

Because the parameter $\alpha + \beta = 0.65$ in CAM-B3LYP, the asymptotic behaviour of the non-AC CAM-B3LYP exchange potential will have the incorrect form $-0.65/r$. Furthermore we find that the non-AC HOMO energies ϵ_h are significantly different from $-I$ (e.g. for C_2H_4, $\epsilon_h = -9.65$ eV (non-AC), compared to $I = 10.60$ eV), although they are significantly improved over GGAs for which $\epsilon_h = -6.69$ eV. Therefore it is appropriate to apply the AC correction; the resultant $\epsilon_h = -10.53$ eV.

3.3. *TDDFT excitation energies for benzene molecule*

The convergence criteria, the smoothing parameters for the nuclear potentials, and the box size are the same as those used in section 3.2. The six core orbitals are frozen in the linear response calculations. The geometries are taken from Handy and Tozer's study [25]. The LSDA, HCTH and CAM-B3LYP exchange-correlation functionals were used.

Table 8 lists the total and HOMO energies and ionization potentials. The excitation energies are given in table 9, which includes the literature values computed by Handy and Tozer [25] along with the reference data [26]. We used the parameters $X = 3.0$ and $Y = 4.0$ for equation (16), while Handy and Tozer used $X = 3.5$ and $Y = 4.7$ [25]. Handy and Tozer's results were obtained using two sets of Gaussian basis functions, 6-31G* and TZ2P, augmented with the double spd (0,01, 0.04) set [25].

In total, the multiresolution TDDFT results are in good agreement with the experimental values. The mean absolute errors for all the states calculated with LSDA, HCTH and CAM-B3LYP were 0.21, 0.12 and 0.18 eV, respectively. Those for the Rydberg excited states are 0.17, 0.06 and 0.14 eV, respectively, which are rather better than those for the valence excited states, 0.27, 0.24 and 0.26 eV, respectively. The most poorly predicted excitation energies are calculated in the 1^3B_{2u} valence excited state, which are in error by around 0.6 eV.

In comparison with Handy and Tozer's Gaussian results using HCTH exchange-correlation functionals [25], we found that their doubly augmented TZ2P Gaussian basis set is adequate for both the computed valence and Rydberg states. The average deviation of the excitation energies calculated with TZ2P and 6-31G* basis sets from the multiresolution ones is 0.05 and 0.14 eV, respectively. The valence excitation energies computed with the TZ2P basis set have a mean absolute error of 0.01 eV.

4. Conclusions

The most sophisticated exchange-correlation functionals can be used in the fully numerical TDDFT solver, so that we are able to compute excitation states of chemical relevance very accurately free of the basis set error (within a controlled accuracy).

The present development provides the following new features in the multiresolution linear response method.

(1) The linear response calculations on the full TD-HF/DFT (i.e. without Tamm–Dancoff approximation) are performed by solving the coupled integral equations iteratively with the BSH kernel being the Green's function.

Table 3. The total, HOMO (ϵ_h) energies, and ionization potential (I) (in hartree) of N_2.

	$k = 7, r(\mathrm{MO}) < 3 \times 10^{-5}$					Tozer *et al.*[c]	Hirata *et al.*[d]		
	LSDA[a]	HCTH[a]	HCTH[b]	CAM-B3LYP[a]	PBE0[a]	HCTH[b]	SVWN	BLYP	Exptl.[e]
Total energy	−108.699 876	−109.544 566		−109.536 553	−109.452 942	−109.518 39	–	–	–
ϵ_h	−0.382 629	−0.378 649		−0.510 291	−0.448 501	–	−0.384 1	−0.377 9	–
I	0.574 131	0.566 314		0.588 286	0.578 337	0.567	–	–	0.572 6
Total energy (AC)	−108.699 801	−109.544 418	−109.544 521	−109.536 521	−109.452 914	−109.518 35	–	–	–
$\epsilon_{h(AC)}$	−0.572 039	−0.563 527	−0.565 164	−0.586 963	−0.577 203	–	−0.611 8	−0.6092	–

[a] The asymptotic correction uses $X = 3.0$, $Y = 4.0$ for equation (16).
[b] The asymptotic correction uses $X = 3.5$, $Y = 4.7$ for equation (16).
[c] From [6]. The basis: augmented Sadlej basis sets.
[d] From [8]. The basis: 6-311(3+, 3+)G**.
[e] From [19].

Table 4. The total, HOMO (ϵ_h) energies, and ionization potential (I) (in hartree) of C_2H_4.

	$k = 7, r(\mathrm{MO}) < 3 \times 10^{-5}$ [a]				Tozer *et al.*[b]
	LSDA	HCTH	CAM-B3LYP	PBE0	HCTH
Total energy	−77.863 098	−78.603 861	−78.575 697	−78.519 234	−78.578 26
ϵ_h	−0.255 545	−0.246 448	−0.340 295	−0.289 974	–
I	0.404 218	−0.388 123	0.387 648	0.385 352	0.390
Total energy (AC)	−77.862 891	−78.603 593	−78.575 653	−78.519 176	−78.578 18
$\epsilon_{h(AC)}$	−0.400 493	−0.384 269	−0.385 994	−0.383 516	–

[a] The asymptotic correction uses $X = 3.0$, $Y = 4.0$ for equation (16).
[b] From [6]. The basis: augmented Sadlej basis sets.

Table 5. Excitation energies (in eV) of Be. The asymptotically corrected exchange-correlations are used.

	$k = 7, r(\mathrm{MO}) < 3 \times 10^{-5}$ [a b]				Tozer *et al.*[b c]	Hirata *et al.*[d]			
	LSDA	HCTH	CAM-B3LYP	PBE0	HCTH	SVWN	BLYP	STEOM CCSD	Exptl.[e]
^1D (2s4d)	8.071	8.111	8.187	8.053	8.20	7.52	7.47	–	8.53
^3D (2s4d)	8.074	8.123	8.183	8.021	8.18	–	–	–	8.42
^3P (2s4p)	7.926	7.962	8.030	7.879	8.07	7.36	7.47	8.31	8.18
^1S (2s4s)	7.788	7.836	7.896	7.762	7.86	7.20	7.20	8.11	8.09
^3S (2s4s)	7.689	7.744	7.791	7.646	7.77	7.12	7.09	8.01	8.00
^1D (2s3d)	7.201	7.271	7.392	7.270	7.30	6.75	6.67	7.72	7.99
^3D (2s3d)	7.272	7.196	7.427	7.190	7.27	6.83	6.71	7.76	7.69
^1P (2s3p)	7.080	7.142	7.220	7.102	7.19	6.61	6.56	7.66	7.46
^3P ($2p^2$)	?	?	?	?	?	?	?	?	7.40
^3P (2s3p)	6.864	6.714	6.993	6.778	6.84	6.41	6.30	7.35	7.30
^1D ($2p^2$)	?	?	?	?	?	?	?	?	7.05
^1S (2s3s)	6.473	6.554	6.610	6.499	6.55	6.02	5.97	6.87	6.78
^3S (2s3s)	6.121	6.105	6.210	6.052	6.11	5.76	5.69	6.51	6.46
^1P (2s2p)	4.915	5.026	4.935	4.984	5.03	4.83	4.86	5.50	5.28
^3P (2s2p)	2.367	2.176	2.036	1.797	2.19	2.36	2.09	2.86	2.73
Error	0.34	0.33	0.26	0.39	0.29	0.65	0.69	0.08	
Max	0.79	0.72	0.69	0.93	0.69	1.24	1.32	0.27	

[a] The computed energies are converged within 10^{-3} eV.
[b] The asymptotic correction uses $X = 3.0$, $Y = 4.0$ for equation (16).
[c] From [6]. The basis: augmented Sadlej basis sets.
[d] From [8]. The basis: 16s11p7d GTOs.
[e] From [20].

(2) GGA and hybrid exchange-correlation functionals as well as LSDA can be used in TDDFT calculations. The second derivative of exchange-correlation functionals is represented fully numerically at $O(N)$ computation cost.
(3) Tozer and Handy's AC is incorporated into the existing exchange-correlation functionals, so that the fully numerical TDDFT calculations yield not only bound states but chemically accurate results, and their computations are numerically stable.
(4) The CAM-B3LYP is implemented in the multiresolution solver. We exploit the separated representation of the attenuated Poisson kernel in the integral operator.

This study demonstrated that the present development could compute reasonably accurate excitation energies on realistic molecules via the TDDFT method using the asymptotically corrected LSDA, HCTH, CAM-B3LYP and PBE0 exchange-correlation functionals. With Tozer and Handy's asymptotic correction, we can consistently calculate the accurate Rydberg excitation energies. For instance, in comparison with the experimental data, the mean absolute deviations of the Rydberg excitation energies of benzene calculated with LSDA, HCTH and CAM-B3LYP exchange-correlation functionals are excellently small, being 0.17, 0.06 and 0.14 eV, respectively.

In the multiresolution calculations, we have no special concern for choosing basis sets. The basis

Table 6. The excitation energies (in eV) of N_2. The asymptotically corrected exchange-correlations are used.

	$k=7, r(\mathrm{MO})<3\times10^{-5}$ [a]					Tozer *et al.*[d]	Hirata *et al.*[e]			
	LSDA[b]	HCTH[b]	HCTH[c]	CAM-B3LYP[b]	PBE0[b]	HCTH[c]	SVWN	BLYP	STEOM CCSD	Exptl.[f]
$^1\Sigma_u^+$	12.807	12.704	12.471	13.212	13.068	12.47	13.25	13.02	12.84	12.98
$^1\Pi_u$	12.696	12.614	12.431	13.066	12.981	12.45	13.30	13.12	12.84	12.90
$^1\Sigma_g^+$	12.046	11.978	11.756	12.560	12.375	11.77	12.62	12.37	12.20	12.2
$^3\Sigma_g^+$	11.667	11.572	11.331	12.071	11.903	11.37	12.21	11.93	11.78	12.0
$^3\Pi_u$	10.454	10.579	10.566	10.774	10.746	10.58	10.42	10.39	11.28	11.19
$^1\Delta_u$	10.26	10.117	10.100	9.696	9.891	10.11	10.34	9.97	10.55	10.27
$^1\Sigma_u^-$	9.705	9.778	9.763	9.228	9.368	9.75	9.76	9.66	10.10	9.92
$^3\Sigma_u^-$	9.705	9.778	9.763	9.228	9.368	9.75	9.76	9.66	9.87	9.67
$^1\Pi_g$	9.105	9.204	9.188	9.397	9.330	9.18	9.16	9.18	9.30	9.31
$^3\Delta_u$	8.94	8.539	8.530	7.897	7.879	8.57	8.92	8.32	8.96	8.88
$^3\Pi_g$	7.663	7.589	7.583	7.702	7.521	7.56	7.62	7.49	8.15	8.04
$^3\Sigma_u^+$	8.178	7.334	7.328	6.978	6.950	7.32	7.94	7.52	7.59	7.75
Error	0.24	0.30	0.37	0.43	0.37	0.36	0.27	0.28	0.13	
Max	0.74	0.61	0.67	0.98	1.00	0.63	0.77	0.80	0.28	

[a] The computed energies are converged within 10^{-3} eV.
[b] The asymptotic correction uses $X=3.0$, $Y=4.0$ for equation (16).
[c] The asymptotic correction uses $X=3.5$, $Y=4.7$ for equation (16).
[d] From [6]. The basis: augmented Sadlej basis sets.
[e] From [8]. The basis: 6-311(3+, 3+)G**.
[f] From [21].

Table 7. The excitation energies (in eV) of C_2H_4. The asymptotically corrected exchange-correlations are used.

	$k=7, r(\mathrm{MO})<3\times10^{-5}$ [a b]				Tozer *et al.*[c]		
	LSDA	HCTH	CAM-B3LYP	PBE0	HCTH	CASPT2[d]	Exptl.[d]
$^1B_{1u}$	9.686	9.288	9.343	9.278	9.32	9.31	9.33
$^1B_{2u}$	9.287	8.937	8.946	8.898	9.04	9.18	9.05
$^1B_{3u}$	9.270	9.057	9.107	9.038	8.95	9.03	8.90
$^1B_{3u}$	8.949	8.691	8.688	8.661	8.70	8.66	8.62
$^3B_{3u}$	8.895	8.583	8.639	8.586	8.64	8.57	8.57
^1A_g	8.737	8.393	8.384	8.338	8.33	8.40	8.28
^3A_g	8.487	8.071	8.128	8.035	8.15	8.26	8.15
$^1B_{1u}$	8.404	8.322	8.262	8.289	7.61	8.40	8.0
$^1B_{2g}$	8.161	7.907	7.926	7.903	7.77	7.95	7.90
$^1B_{1g}$	8.117	7.890	7.831	7.838	7.78	7.85	7.80
$^3B_{1g}$	8.072	7.812	7.790	7.802	7.76	7.80	7.79
$^1B_{3u}$	7.429	7.280	7.198	7.217	7.16	7.17	7.11
$^3B_{3u}$	7.332	7.190	7.101	7.081	7.10	7.05	6.98
$^3B_{1u}$	4.807	4.468	4.103	4.064	4.33	4.39	4.36
Error	0.34	0.11	0.10	0.10	0.07	0.09	
Max	0.46	0.32	0.26	0.30	0.39	0.40	

[a] The computed energies are converged within 10^{-3} eV.
[b] The asymptotic correction uses $X=3.0$, $Y=4.0$ for equation (16).
[c] From [6]. The basis: augmented Sadlej basis sets. The asymptotic correction uses $X=3.5$, $Y=4.7$ for equation (16).
[d] From [22].

errors are adaptively refined, so that we can efficiently and consistently obtain arbitrary numerical accuracy of the excitation energies on either valence or Rydberg excitations. The numerical accuracy of linear response properties such as excitation energies is in proportion to the residual norms of molecular orbitals and response functions in the integral equations.

Table 8. The total, HOMO (ϵ_h) energies, and ionization potential (I) (in hartree) of benzene.

	$k = 7, r(\text{MO}) < 3 \times 10^{-5}$ [a]		
	LSDA	HCTH	CAM-B3LYP
Total energy	−230.202 607	−232.260 841	−232.213 237
ϵ_h	−0.240 628	−0.230 432	−0.313 256
I	0.351 704	−0.337 757	0.341 892
Total energy (AC)	−230.202 290	−232.260 421	−232.213 198
$\epsilon_{h(AC)}$	−0.348 140	−0.333 943	−0.340 658

[a] The asymptotic correction uses $X = 3.0$ and $Y = 4.0$ for equation (16).

Table 9. The excitation energies (in eV) of benzene.

	$k = 7, r(\text{MO}) < 3 \times 10^{-5}$ [a b]			Handy *et al*/HCTH[c]		
	LSDA	HCTH	CAM-B3LYP	6-31G*	TZ2P	Exptl./CASPT2*[d]
Valence excitations						
1^3B_{1u}	4.408	4.019	3.595	4.11	4.02	3.94
1^3E_{1u}	4.757	4.651	4.781	4.78	4.66	4.76
1^1B_{2u}	5.276	5.283	5.489	5.44	5.28	4.90
1^3B_{2u}	5.006	4.977	5.088	5.15	4.98	5.60
1^1B_{1u}	6.045	6.006	6.158	6.24	6.02	6.20
1^1E_{1u}	6.895	6.912	7.012	7.00	6.94	6.94
Rydberg excitations						
1^1E_{1g}	6.529	6.404	6.504	6.15	6.24	6.334
1^1A_{2u}	6.885	6.992	7.221	6.81	6.92	6.932
1^1E_{2u}	6.980	6.980	7.109	6.79	6.90	6.953
1^1A_{1u}	7.004	6.990	7.014	6.81	6.91	6.99*
2^1E_{1u}	7.426	7.360	7.297	7.34	7.24	7.41
1^1B_{1g}	7.783	7.546	7.702	7.39	7.50	7.460
1^1B_{2g}	7.811	7.561	7.715	7.41	7.52	7.460
2^1E_{1g}	7.614	7.451	7.539	7.41	7.52	7.535
1^1E_{2g}	8.071	7.729	7.874	7.66	7.76	7.81
2^1A_{1g}	8.085	7.747	7.924	7.63	7.80	7.81
1^1A_{2g}	8.079	7.746	7.877	7.63	7.78	7.81
Mean absolute deviations						
Valence	0.27	0.24	0.26	0.21	0.22	
Rydberg	0.17	0.06	0.14	0.13	0.06	
Total	0.21	0.12	0.18	0.16	0.12	
Maximum absolute deviation						
Valence	0.59	0.62	0.59	0.54	0.62	
Rydberg	0.35	0.10	0.29	0.18	0.17	
Total	0.59	0.62	0.59	0.54	0.62	

[a] The computed energies are converged within 10^{-3} eV.
[b] The asymptotic correction uses $X = 3.0$ and $Y = 4.0$ for equation (16).
[c] The asymptotic correction uses $X = 3.5$ and $Y = 4.7$ for equation (16). The basis sets are augmented with the double spd (0.01, 0.04) set.
[d] From [26].

Acknowledgments

We thank Dr David J. Tozer for providing us with his program subroutine, a part of CADPAC, for the Tozer–Handy asymptotic correction. RJH and TY were funded by the Scientific Discovery through Advanced Computing (SciDAC) program of the US Department of Energy, the division of Basic Energy Science, Office of Science, under contract DE-AC05-00OR22725 with Oak Ridge National Laboratory.

This research was performed in part using the resources of the Center for Computational Sciences at Oak Ridge National Laboratory under contract DE-AC05-00OR22725.

NWChem Version 4.5, as developed and distributed by Pacific Northwest National Laboratory, PO Box 999, Richland, Washington 99352 USA, funded by the US Department of Energy, was used to obtain the HF, DFT and TD-HF/DFT results.

The Coulomb-attenuating DFT exchange-correlation functional was evaluated using DFT functional sub-routines implemented in UTChem 2004, University of Tokyo, Tokyo, Japan.

References

[1] R.J. Harrison, G.I. Fann, T. Yanai, Z. Gan, G. Beylkin, *J. Chem. Phys.*, (in the press) (2004).
[2] T. Yanai, G.I. Fann, R.J. Harrison, G. Beylkin, *J. Chem. Phys.*, submitted (2004).
[3] T. Yanai, G.I. Fann, Z. Gan, R.J. Harrison, G. Beylkin, *J. Chem. Phys.*, **121,** 2866 (2004).
[4] T. Yanai, G.I. Fann, Z. Gan, R.J. Harrison, G. Beylkin, *J. Chem. Phys.*, **121,** 6680 (2004).
[5] T. Yanai, R.J. Harrison, *J. Chem. Phys.*, submitted (2004).
[6] D.J. Tozer, N.C. Handy, *J. Chem. Phys.*, **109,** 10180 (1998).
[7] T. Yanai, D.P. Tew, N.C. Handy, *Chem. Phys. Lett.*, **393,** 51 (2004).
[8] S. Hirata, S. Ivanov, I. Grabowski, R.J. Bartlett, *J. Chem. Phys.*, **116,** 6468 (2002).
[9] R.G. Parr, W. Yang, *Density-Functional Theory of Atoms and Molecules*, Oxford University Press, New York (1989).
[10] D.J. Tozer, R.D. Amos, N.C. Handy, B.O. Roos, L. Serrano-Andres, *Molec. Phys.*, **97,** 859 (1999).
[11] A.D. Becke, *J. Chem. Phys.*, **98,** 5648 (1993).
[12] P.J. Stephens, J.F. Devlin, C.F. Chabalowski, M.J. Frisch, *J. Chem. Phys.*, **98,** 11623 (1993).
[13] H. Iikura, T. Tsuneda, T. Yanai, K. Hirao, *J. Chem. Phys.*, **115,** 3540 (2001).
[14] Y. Tawada, T. Tsuneda, S. Yanagisawa, T. Yanai, K. Hirao, *J. Chem. Phys.*, **120,** 8425 (2004).
[15] M. Abramowitz, I.A. Stegun (eds), *Handbook of Mathematical Functions*, section 25.4.7, p. 886, Dover Publications, New York (1965).
[16] F.A. Hamprecht, A.J. Cohen, D.J. Tozer, N.C. Handy, *J. Chem. Phys.*, **109,** 6264 (1998).
[17] R.A. Kendall, J.T.H. Dunning, R.J. Harrison, *J. Chem. Phys.*, **96,** 6769 (1992); J.T.H. Dunning, *J. Chem. Phys.*, **90,** 1007 (1989); A.K. Wilson, T.v. Mourik, J.T.H. Dunning, *J. Molec. Struct. (THEOCHEM)*, **388,** 339 (1997); D.E. Woon, J.T.H. Dunning, *J. Chem. Phys.*, **98,** 1358 (1993); D.E. Woon, J.T.H. Dunning, *J. Chem. Phys.*, **100,** 2975 (1994).
[18] High Performance Computational Chemistry Group, *NWChem, A Computational Chemistry Package for Parallel Computers, Version 4.5*, Pacific National Laboratory, Richland, Washington 99352, USA (2003).
[19] P.J. Linstrom, W.G. Mallard (eds), *NIST Chemistry Web Book, NIST Standard Reference Database Number 69*, National Institute of Standards and Technology, Gaithersburg, MD (2001) (http://webbook.nist.gov/).
[20] R.L. Graham, D.L. Yeager, J. Olsen, P. Jolgensen, R. Harrison, S. Zarrabian, R. Bartlett, *J. Chem. Phys.*, **85,** 6544 (1986).
[21] S.B. Ben-Shlomo, U. Kaldor, *J. Chem. Phys.*, **92,** 3680 (1990).
[22] L. Serrano-Andres, M. Merchan, I. Nebot-Gil, R. Lindh, B.O. Roos, *J. Chem. Phys.*, **98,** 3151 (1993).
[23] D.J. Tozer, N.C. Handy, *Phys. Chem. Chem. Phys.*, **2,** 2117 (2000).
[24] C. Adamo, V. Barone, *J. Chem. Phys.*, **110,** 6158 (1999).
[25] N.C. Handy, D.J. Tozer, *J. Comput. Chem.*, **20,** 106 (1999).
[26] J. Lorentzon, P.-A. Malmquist, M. Fulscher, B.O. Roos, *Theor. Chim. Acta.*, **91,** 91 (1995).